FTIR Imaging of the Dissolution of Polymers. 4. Poly(methyl methacrylate) Using a Cosolvent Mixture (Carbon Tetrachloride/ Methanol)

J. González-Benito† and J. L. Koenig*,‡

Department of Materials Science and Metallurgic Engineering, Universidad Calos III de Madrid, Avda, Universidad 30, 28911 Leganés, Madrid, Spain, and Department of Macromolecular Science, Case Western Reserve University, Cleveland, Ohio 44106

Received March 15, 2002

ABSTRACT: The dissolution process of poly(methyl methacrylate) in mixtures of methanol and carbon tetrachloride, individually nonsolvents for the polymer (under the conditions of study), was studied at 25 °C using FTIR imaging spectroscopy. To investigate this cosolvency phenomenon, the spatial resolution and sensitivity of FTIR imaging to interactions between the components were used. The results obtained suggest that the dissolution process of the PMMA in a high weight fraction of the CCl_4/CH_3OD solvent mixtures consists of first the swelling of the PMMA by the CCl_4 allowing the methanol to penetrate into the PMMA and specifically interact (hydroxyl−carbonyl hydrogen bonds) with the polymer to separate the polymer chains. Furthermore, the effect of compositions of the solvent mixtures on the dissolution rates is a result of two opposite effects: (i) the ability of the polymer to be swelled (CCl_4 fraction) and (ii) the number of specific interactions between the polymer and one of the nonsolvents (methanol fraction).

1. Introduction

Polymer dissolution in a solvent is an important phenomenon in a variety of applications. The semiconductor industry has an interest in controlling the dissolution rate of resist films. Many electron beam resists are based on PMMA, and the development of the lithography pattern is achieved by the use of mixtures of alcohols and ketones. Alcohols are nonsolvents for PMMA, whereas ketones are good solvents. During the exposure process, the high molar mass polymer undergoes progressive chain scission producing a lower molar mass product. Changes in the solvent mixture and temperature result in the mixture changing from being a good to a poor solvent for the polymer. Since solubility is a function of molar mass, it is possible to select a mixture which will selectively dissolve the low molar mass components without significantly swelling the unexposed, higher molar mass components.

A good alternative to the solvent/nonsolvent mixture might be a nonsolvent/nonsolvent mixture, since it may be even less sensitive to the swelling process of the higher molar mass components. In 1920s, it was found that two nonsolvents for a polymer, when mixed in specific compositions, can actually function as a solvent for that polymer; this phenomenon has been named cosolvency. It has been reported that the cosolvent effect can be very useful in order to control the mesostructure of the polymers. Coutinho et al.[1] obtained for styrene−divinylbencene copolymers collapsed-type structures by using cosolvent mixtures and macroporous ones when the pure solvents were employed as diluents.

PMMA has been reported to dissolve in several nonsolvent pairs, including benzyl alcohol/*sec*-butyl chloride, tetrachloromethane/*tert*-butyl chloride, tetrachloromethane/butyl chloride,[2] and CCl_4 with several alcohols (MeOH, EtOH, PrOH, and BuOH).[3] Fernández-Piérola et al.[4] reported other mixtures based mainly on acetonitrile that act as cosolvents of the PMMA. Cowie et al.[5] reported the cosolvency of PMMA in dilute solutions (3% w/v) of water and various alcohols, and Cheng et al.[6] reported the phase behavior of a water/2-propanol/PMMA cosolvent system.

The cosolvency phenomenon is not very well understood.[4,5,7,8] The easiest way to understand this dissolution behavior is by making use of the simple solubility parameter (δ) theory. Consider an ideal cooperative effect between the nonsolvents and assume that the mixture of solvents can be treated as an intermediate liquid having individual contributions to the δ value (dispersion forces, δ_d, dipolar interactions, δ_p, and hydrogen bonding, δ_h, contributions) equal to the averages of the δ's of the two liquids.[4] Nevertheless, some of the cosolvent systems, such as water/2-propanol[5,6] and formamide/ethanol,[4] do not fit this approximation, and this suggests that there must be another explanation for the cosolvency, at least for these systems.

However, as always, when a process is under study, it is necessary to take into account not only the thermodynamic criteria but also the kinetics. In general, solvent mobility is primarily related to its molecular size whereas thermodynamic compatibility is associated with the strength of the interactions between structural groups of the polymer and solvent molecules. There are several works related to the study of the dissolution process of polymers; all of them account for the solvent penetration and dissolution to be controlled kinetically.[9−11] In fact, for some applications it is of primary importance to control the rate of the dissolution process. In general, it is proposed[11] that solvent penetration is the first step of polymer dissolution. The solvent enhances the mobility of polymer chains by converting the glassy matrix to a swollen, rubbery material. If the solvent and polymer are thermodynamically incompatible, then only swelling will be observed. However, if the solubility parameters are similar, polymer chains at the

† Universidad Calos III de Madrid.
‡ Case Western Reserve University.
* To whom correspondence should be addressed.

10.1021/ma020401u CCC: $22.00
Published on Web 08/16/2002

polymer−solvent interface will disentangle from the swollen matrix. Several limiting cases of dissolution can be envisioned, depending on the relative kinetics of solvent penetration, chain disentanglement, and external mass transfer. If external mass transfer is assumed to be rapid, the degree of swelling during dissolution depends on the relative rates of penetration and disentanglement. When penetration is rapid relative to disentanglement, an appreciable swollen surface layer forms, whereas minimal surface swelling is observed when the chains rapidly disentangle as the solvent permeates.

Solvent or nonsolvent diffusion in glassy polymers is often characterized by a constant penetration velocity. This non-Fickian behavior, termed case II diffusion,[12,13] is controlled by polymer relaxation and is characterized by a front of constant penetrant composition that invades the glassy polymer at a constant rate. For nonsolvent penetration, concentration in the solvent swollen gel layer remains constant, and the mass uptake is linear with time. In the case of strong solvents, the gel layer rapidly dissolves into the solvent, and its thickness is typically not detectable. Thus, with strong solvents, case II diffusion gives rise to a constant dissolution rate.

A number of instruments have been developed for the measurement of diffusion and/or dissolution rates. The most direct way to properly characterize the diffusion and/or dissolution processes is to determine both the swelling of the polymer and concentration spatial profiles of the penetrant and their time-dependent behavior. A laser interferometric technique has been used to investigate diffusion of methanol in PMMA,[14,15] obtaining the volume fraction of MeOH in the swollen layer behind the moving front, the steady-state front speed (diffusion rate when case II transport is concerned), and the characteristic induction time. However, this technique does not allow determination of the concentration profiles. Pekan et al.[16−18] have studied the dissolution process of fluorescence labeled PMMA samples by monitoring the fluorescence of the dissolved residues during its incorporation to the solution. But, in this case, it is not possible to obtain concentration profiles, and one cannot study the interactions of the polymer with the solvent as it dissolves. Several techniques such as ATR−FTIR,[19] NMR imaging,[20] and fluorescence nonradiative energy transfer (NRET)[21] have been used to determine the concentration profiles in diffusing systems. NRET has the advantage of requiring no specialized equipment and has a fast time resolution, but it requires fluorescing acceptor and donor moieties in the system that may inadvertently affect the diffusion and, therefore, the dissolution processes. NMR imaging possesses relatively fast time resolution but is limited by the spatial resolution and, in the chemical systems that can be studied, because this technique uses differences in molecular mobility to differentiate between components. Classical FTIR microspectroscopy has the advantages of extremely high chemical specificity but is limited by its inherently low spatial resolution and long collection times, which does not allow studying relatively fast phenomena. On the contrary, FTIR imaging uses a focal plane array (FPA) and has faster acquisition times and higher resolution.[22] In addition, FTIR imaging allows the detection of initial chemical or physical imperfections in the sample being studied and those generated during the diffusion process.

The aim of this work is to study the effect of the carbon tetrachloride/methanol cosolvent mixture compositions on the PMMA dissolution as reflected in the rate of this process. With FTIR imaging, one can measure the composition profiles as a function of time for the components in the system and any interactions between them.

2. Experimental Section

Atactic PMMA with molecular weight M_w = 12 000 g/mol and polydispersity ~ 2 was used as received from Aldrich Chemical Co., Milwaukee, WI. Carbon tetrachloride (CCl_4) and methyl alcohol-*d* (CH_3OD) were supplied by Aldrich Chemical Co., Milwaukee, WI, and used as receive without further purification. For the sample used and under the conditions of our study, these liquids were proved to be nonsolvent of the PMMA as FTIR experiments reflected, which is in accordance with reported data.[23] Experiments were conducted using the contact method.[24] To prepare a thin layer of polymer sandwiched between two salt plates, a solution of 10% (w/w) of PMMA in chloroform was prepared. After that, a small drop of the solution was placed on a 2 mm thick CaF_2 substrate and then remained at room temperature for 30 min to remove the solvent. Another substrate was then placed on top of the polymer, and the two plates were clamped together and heated on an oven to 200 °C for 2 h. After that, it was allowed to cool in ambient air to room temperature. The clamps were removed to yield a polymer film with 5 μm of thickness partially occupying space between the two plates. The dissolution experiments were performed by introducing the solvent or the mixture of solvents from the empty end after the sample interface was positioned in the spectrometer. The solvent entered the space between the substrates due to capillary action and came into contact with the polymer; at that moment it was considered that the dissolution process started. Great care to have good sample contact with the optical windows was taken, and the resulting images (in the polymer zone) showed no solvent behind the dissolution interface. FTIR images were sequentially acquired during the dissolution time in the region of view in which is included the polymer/solvent system interface. Solvent was added as necessary.

To study the effect of the solvent mixture composition on the dissolution rate of PMMA, seven solutions of CCl_4 + CH_3OD were prepared with 0, 10, 20, 30, 40, 50, and 100% (w/w) of CH_3OD.

Infrared images were collected using a Bio-Rad Stingray imaging spectrometer (Digilab Laboratories, Cambridge, MA). The Stingray is comprised of an FTS6000 step-scan interferometer bench coupled to a microscope accessory, UMA-500. The imaging detector used is a Santa Barbara focal plane FPA consisting of a 64 × 64 array of mercury cadmium telluride (MCT) elements imaging and average spatial area of 400 × 400 μm. A long pass filter to eliminate unwanted wavelengths and prevent Fourier fold-over perturbations was inserted into the beam path. The spectral region recorded was from 1000 to 4000 cm^{-1}. Furthermore, an 8 cm^{-1} nominal spectral resolution and an undersampling ratio (UDR) of 4 were used for the study. A mirror stepping rate of 5 Hz was used, yielding a total scanning time of about 300 s. The number of camera frames (frame rate = 316 Hz) averaged during each spectrometer step was 24. Image processing and data extraction were carried out using the hyperspectral imaging software package Environment for Visualizing Images (ENVI) (Research Systems Inc.). Lower noise absorbance profiles were extracted from each image by averaging spectra stored in an image region of 5 pixels perpendicular to the dissolution direction.

3. Results and Discussion

To analyze each component of the system (polymer/solvent) separately, one uses their characteristic IR spectra. Normally, it is possible to find, at least, one

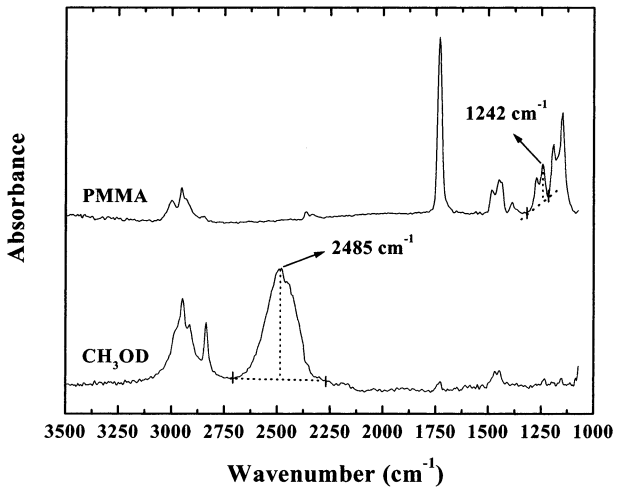

Figure 1. FTIR spectra of the system components. The absorbance was obtained from the heights of the peaks after doing proper baseline correction.

peak which is characteristic of each component. Therefore, once the peaks are selected, their absorbance values can be followed whatever the region of the image was selected. Figure 1 shows the FTIR spectra for the PMMA and CH_3OD. The FTIR spectrum for the CCl_4 has not been represented because in the IR region of study it only appears as a very low absorbance peak assigned to the C−Cl stretching overtone (1585 cm^{-1}). This very low absorbance only allows a limited analysis of the CCl_4 component as a function of the diffusion process in the case of using it as a pure solvent. However, as can be seen in Figure 1, the CH_3OD band centered at 2490 cm^{-1} and assigned to O−D stretching mode does not overlap with any of the PMMA bands, while the PMMA band centered at 1242 cm^{-1} assigned to the $-CH_2$ bending mode does not overlap with any of the CH_3OD bands. Therefore, these two bands are good choices for monitoring selectively both components in the region of study. Chemically specific images for PMMA and CH_3OD within the system were obtained by plotting the absorbance of the selected IR peaks in each pixel of the FPA. Each absorbance value is associated with a false color in order to see the images as a gradient of colors indicating the distribution of the components in the image. In Figure 2 an example of the variation of this image as a function of the PMMA dissolution process when the solvent mixture composition is 20% (w/w) in CH_3OD is shown. In this way, it is possible to have not only spatial data but also chemical information associated with it.

In Figure 2, the PMMA chemical response reflects the polymer interface movement as a function of the polymer−solvent contact time. The same observations were made for the rest of the solvent mixture compositions studied except for the pure solvents (for which, practically, there is no dissolution of the polymer). This result is in accordance with the cosolvent behavior observed in the CCl_4−CH_3OH/PMMA system.[3] In addition to this, the absorbance of CH_3OD in the images suggests that its front moves with the polymer interface. However, there is not an exact coincidence in the polymer/solvent limit as can be seen in paired of images for each dissolution time. The CH_3OD front seems to be ahead of the images of the PMMA interface (Figure 3). This result suggests that CCl_4 may penetrate first the PMMA in order to swell the polymer. In fact, comparing the images when the experiment was carried out with pure CCl_4 with those with CCl_4/CH_3OD mixtures, it is observed, in the first case, the limit of the solvent interface coincides with the polymer interface, while in the second case this does not happens (Figure 3). All of these observations suggest that CCl_4 swells the PMMA and allows the CH_3OD to penetrate and specifically interact with the polymer and then attain the conditions required for dissolution. Cowie et al.[5] proposed that for the cosolvent system 2-propanol/water/PMMA, although water is a harsh nonsolvent for PMMA, there are possible specific site interactions between PMMA (carbonyl group) and water in a like-contacting-like manner or even via hydrogen bonding. Shimizu et al.[25] using small-angle neutron and X-ray scattering measurements calculated for the same cosolvent system the contributions of the segment−segment interactions to the entropy and enthalpy. On the basis of the negative values obtained for the entropy, they concluded that the water molecules do not form the cagelike water structure around PMMA. They explained the dissolution of PMMA into 80% 2-propanol aqueous solvent as due to hydrogen bonding between water molecules and the C═O group of PMMA. Taking into account that methanol is an important hydrogen-bonding molecule, although weaker than water, one may use these arguments to explain the specific interactions between PMMA and methanol.

It is well-known that the IR carbonyl band centered at 1730 cm^{-1} shifts to lower wavenumbers when the carbonyl group is hydrogen bonded. Therefore, in the case of hydrogen bonding between the carbonyl group of the PMMA and the hydroxyl of the methanol, it should be able to observe this spectral shift with the analysis of the FTIR spectra of the region in which the PMMA is dissolved or partially dissolved by the solvent mixture. To study this, the system with a cosolvent composition of 50% in CH_3OD was selected. From the image obtained at the longest dissolution time studied two spectra were extracted, one of the polymer bulk region and the other of the polymer/solvent interface region. Then the carbonyl band was selected for subsequent analysis (Figure 4). Figure 4 shows that the carbonyl band has a weak contribution at lower wavenumbers when the polymer is directly in contact with the solvent mixture. This result indicates that a strong interaction between PMMA and methanol via hydrogen bonding exists. To see the effect of the different compositions in this interaction, subtraction of the normalized bands in Figure 4 was made. The wavenumbers corresponding to the minimum (1750 cm^{-1}) and the maximum (1711 cm^{-1}) values were taken for analyzing their absorbance variations along the dissolution direction in all of the samples under study. Figure 5 shows the absorbance profiles for these two wavenumbers. In all of the cases, except when pure CCl_4 is used as the solvent, the absorbance at the lower wavenumber is more intense near the polymer/solvent mixture interface. This result confirms the presence of hydrogen bonding in every system with methanol. On the other hand, comparing the plots for the different compositions, it is observed that the differences between the absorbances of the lower and higher wavenumber band after the interface in the solvent region increase with the CH_3OD concentration. This observation indicates that, as expected, an increase in the number of hydroxyl groups yields more hydrogen bondings.

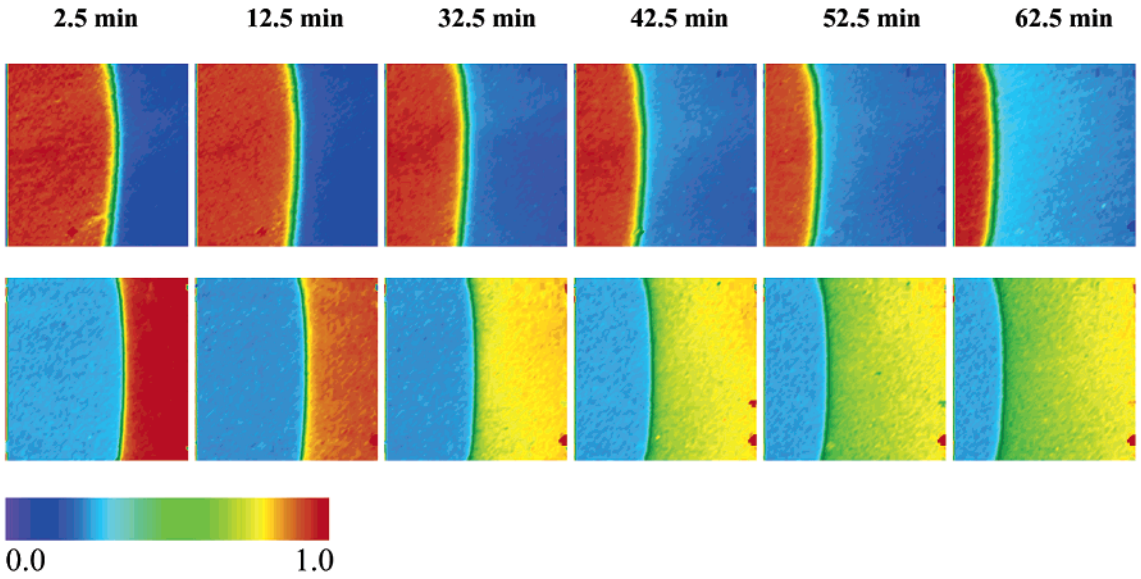

Figure 2. Images of PMMA (top) and CH_3OD (bottom) evolution during one dissolution study in the CCl_4/CH_3OD solvent mixture with a composition of 20% (w/w) CH_3OD.

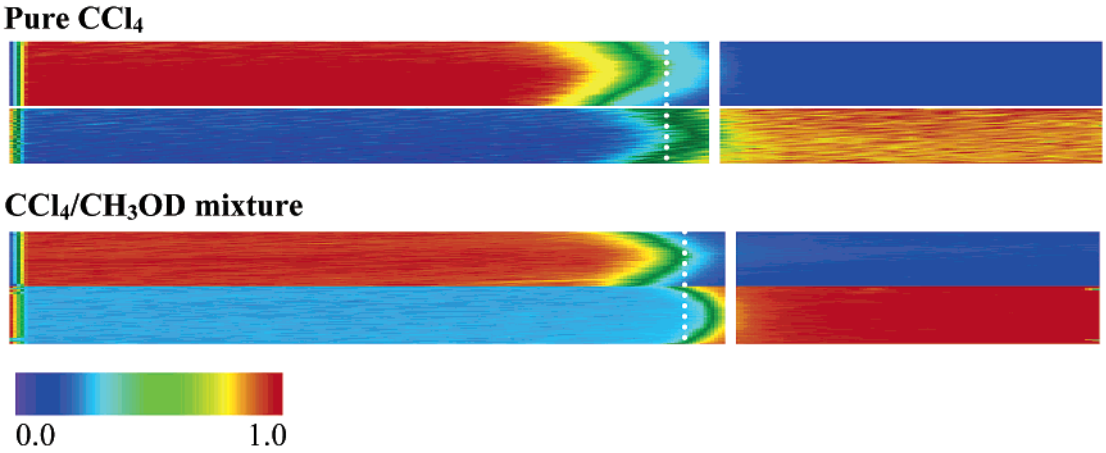

Figure 3. Comparison between the images obtained when the experiment was carried out with pure CCl_4 and those with CCl_4/CH_3OD mixtures. The images were size changed (horizontally stretched) for better visualizing the comparison.

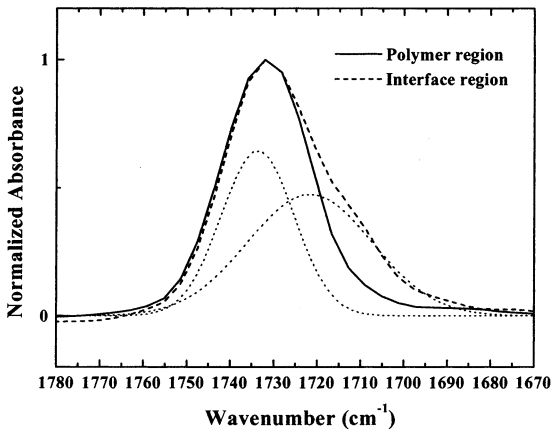

Figure 4. Normalized carbonyl band of the PMMA in the polymer bulk region (whole line) and in the polymer/solvent mixture interface region (dashed line). The dotted lines are the double Gaussian fit to separate hydrogen-bonding contribution.

On the other hand, from all of the images, it is possible to obtain the concentration profiles for the PMMA and CH_3OD components by extracting the absorbances of the characteristic IR peaks along the dissolution direction. The terms absorbance profile and concentration profile will be use interchangeably throughout this paper. This relationship is discussed in more detail elsewhere.[26,27]

As an example, Figure 6 shows several FTIR spectra used in extracting the concentration profiles, while Figure 7 shows the normalized absorbance profiles for PMMA and CH_3OD as a function of the dissolution time when the CCl_4/CH_3OD solvent mixture is 20% in CH_3OD. Therefore, Figure 7 reflects the concentration profiles for the PMMA and the CH_3OD extracted from the images of Figure 2. The rest of the systems studied (other solvent mixture compositions) showed similar results. All of the concentration profiles show similar behavior, a maximum absorbance in the region of the component bulk, a sharp absorbance decrease in the solvent/polymer interface, and finally no absorbance for the solvent in the bulk polymer region and a weak absorbance, which depends on the system, for the polymer in the bulk solvent region. The last observation shows that after dissolution the polymer can diffuse through the solvent but without having the possibility of being removed completely as no stirring occurred.

The dissolution rates were calculated from the absorbance profiles, first, as the polymer interface moved

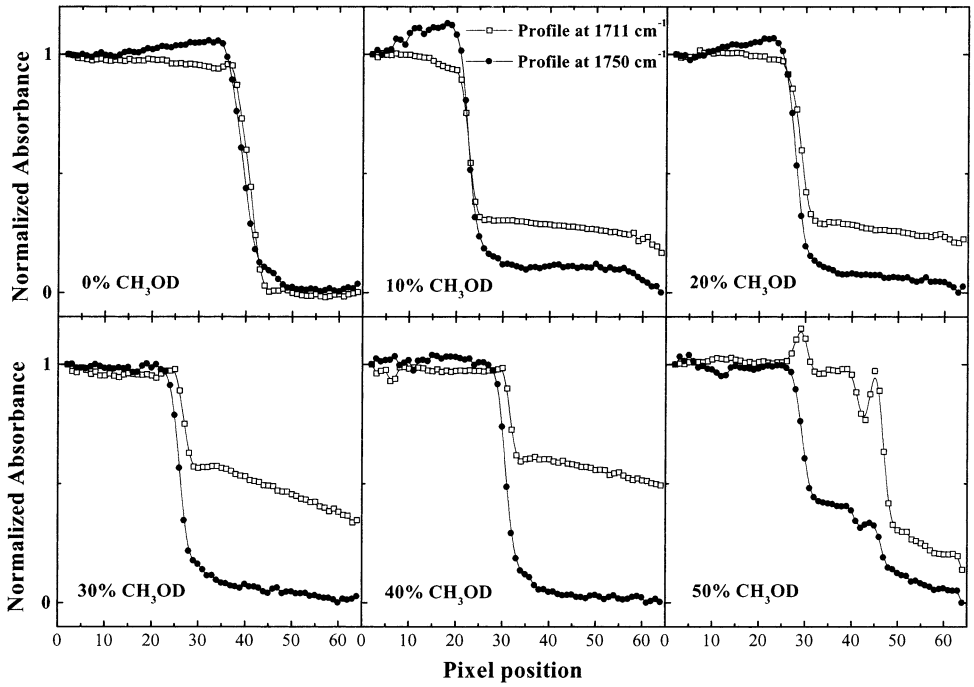

Figure 5. Absorbance profiles at the lower and higher wavenumber of the IR carbonyl signal.

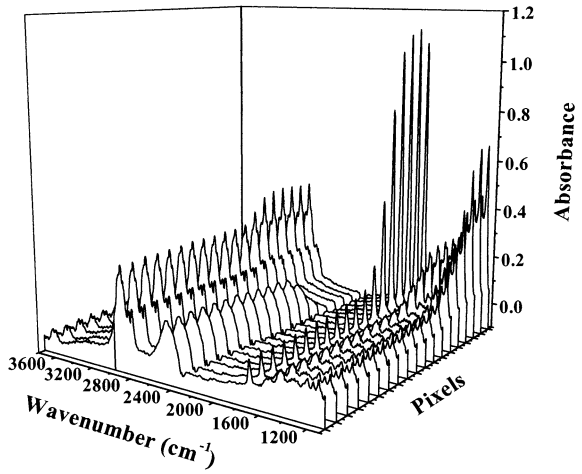

Figure 6. 3D representation of several FTIR spectra used in extracting the concentration profiles (solvent mixture concentration = 20% in CH_3OD, dissolution time = 27.5 min).

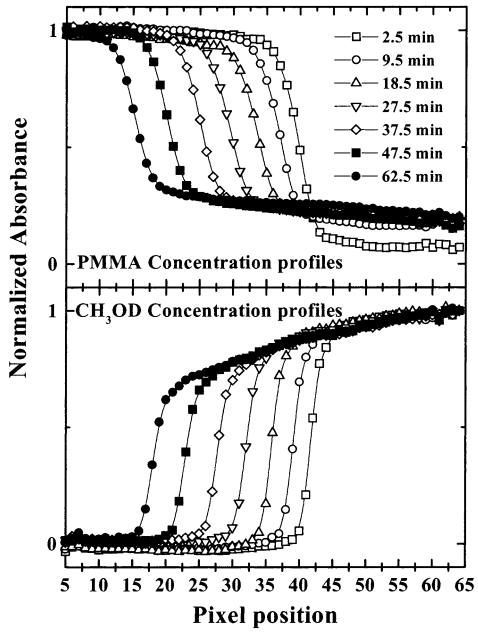

Figure 7. PMMA and CH_3OD concentration profiles obtained at different dissolution times.

with time and, second, as the solvent front moves with time; in both cases the rates were the same. To improve the accuracy in taking the values of the interface position, differentiation of the absorbance profiles was done, and the maxima or minima were used. Therefore, the polymer/solvent interface was plotted as a function of time to determine the dissolution rate. Figure 8 shows this plot for all the compositions studied. The position of the interface was translated into microns considering that each pixel in the images corresponds to 6.25 μm. All plots of Figure 8 can be fit by straight lines with correlation factors higher than 0.995. The first conclusion that can be extracted from this result is that the solvent diffusion follows a case II behavior characterized by a constant penetration velocity (see Introduction).

The polymer dissolution rate as a function of CCl_4/CH_3OD solvent mixture composition is represented in Figure 9. It is observed that the polymer was not dissolved when pure CCl_4 is used as pure solvent while, as the proportion of CH_3OD in the solvent mixture increases, the dissolution rate increases, showing a maximum at about 21% (w/w) of methanol in the solvent mixture. After that composition, the dissolution rates decrease gradually with a lower slope up to 100% of methanol in which there is no dissolution of the polymer. Qualitatively, this cosolvency effect may be explained in thermodynamic terms. The quality of a solvent toward the dissolution of a polymer should be the higher the lower difference in the solubility parameter, δ. In the case of mixed solvents, it is usually assumed that the mixture can be treated as an intermediate liquid having a δ value, which is the average between those from each component. In addition to this, if one considers δ decomposed into contributions from dispersion forces, δ_d, dipolar interactions, δ_p, and hydrogen bonding or other specific forces, δ_h, it could be

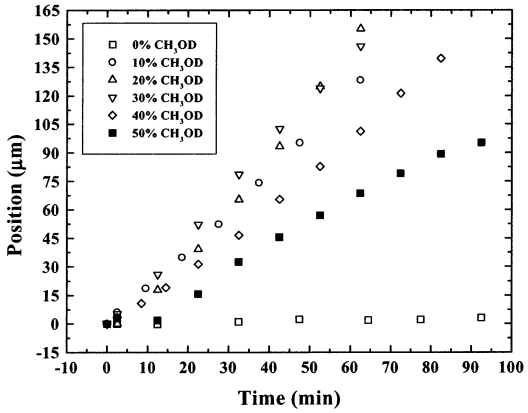

Figure 8. Evolution of the PMMA/CCl_4−CH_3OD interface position as a function of the dissolution time.

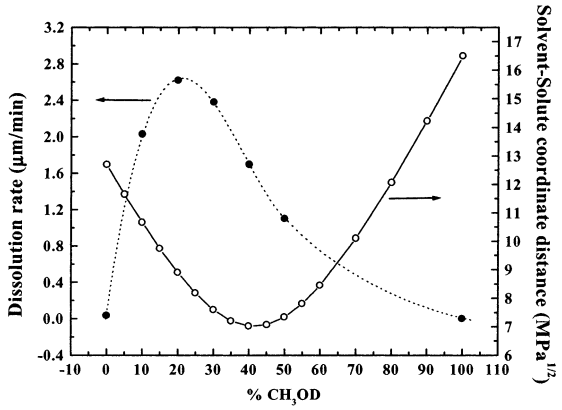

Figure 9. Polymer dissolution rate (left) and the calculated values of the distance between solvent and solute coordinates, R_{ij} (right), as a function of CCl_4/CH_3OD solvent mixture composition.

assumed that these contributions also can be averaged in the case of solvent mixtures. In this way, a region of solubility has been characterized by the distance between solvent and solute coordinates.[28]

$$R_{ij} = [4(\delta_{1d} - \delta_{2d})^2 + (\delta_{1p} - \delta_{2p})^2 + (\delta_{1h} - \delta_{2h})^2]^{1/2} \quad (1)$$

where subscript 1 indicates the solvent and subscript 2 the solute (the polymer). Therefore, the greater the R_{ij} is the lower solubility of the polymer. In Figure 9 it was also plotted the calculated value of R_{ij} as a function of weight percentage of CH_3OD in the solvent mixture, averaging each contribution to the solvent mixture solubility parameter. First, as the methanol proportion increases, there is a decrease in R_{ij} and therefore a solubility increase of the polymer. Second, it reaches a minimum (maximum solubility), and finally there is a decrease in R_{ij}. Thus, qualitatively there is a correspondence in behaviors between dissolution velocity and solubility power. However, the maximum dissolution rate does not correspond with the maximum ability of the polymer to be dissolved. One must take into account the kinetic aspects associated with the diffusion process of the solvents. For this study, the same comparisons were made with different systems studied by other authors,[10,26,27,29] and similar results were obtained, independent of whether the solvents used were good for the polymer or not. This study with other systems allows generalizing the cosolvency as the synergic effect generated by a solvent mixture with respect to the solubility of a solute.

To explain why the dissolution process is faster at methanol concentrations smaller than those thermodynamically expected, it is necessary to consider the dissolution process of the PMMA in the CCl_4/CH_3OD solvent mixtures as follows. The process consists of the swelling by the CCl_4, which allows the methanol to penetrate the PMMA and specifically interact with it to separate the macromolecular chains. In this case, there are two opposite effects with respect to the dissolution velocity: first, the ability of the polymer to be swelled (CCl_4 proportion) and, second, the number of specific interactions between the polymer and the solvent (methanol proportion).

4. Conclusions

By utilizing FTIR imaging, it was possible to acquire not only spatial data but also selective chemical information in the system CCl_4−MeOD solvent mixture/PMMA. Form this study, the CCl_4/MeOD was confirmed to be a cosolvent system of PMMA. Furthermore, the results obtained suggest that the dissolution process of the PMMA in a large range of weight fractions of the CCl_4/CH_3OD solvent mixtures consists of first the swelling of the PMMA by the CCl_4, allowing the methanol to penetrate into the PMMA and specifically interact (hydroxyl−carbonyl hydrogen bonds) with the polymer to separate the polymer chains. Finally, the effect of compositions of the solvent mixtures on the dissolution rates is a result of two opposite effects: (i) the ability of the polymer to be swelled (CCl_4 fraction) and (ii) the number of specific interactions between the polymer and one of the solvents (methanol fraction).

Acknowledgment. The authors acknowledge the Education, Culture and Sports Ministry of Spain for supporting the post-doc study of Dr. J. Gonzalez-Benito at the Department of Macromolecular Science (Case Western Reserve University, Cleveland, OH). J.L.K. acknowledges the support of the Polymer Section of the Division of Materials at NSF DMR0100428.

References and Notes

(1) Coutinho, F. M. B.; Torre, M. L.; Rabelo, D. *Eur. Polym. J.* **1998**, *34*, 805−808.
(2) Kamide, K. In *Thermodynamics of Polymer Solutions, Phase Equilibria and Critical Phenomena*; Elsevier: Amsterdam, 1990; Chapter 3, pp 303−309.
(3) Deb, P. C.; Palit, S. *Makromol. Chem.* **1973**, *166*, 227.
(4) Fernández-Piérola, I.; Horta, A. *Makromol. Chem.* **1981**, *182*, 1705−1714.
(5) Cowie, J. M. G.; Mohsin, M. A.; McEwen, I. J. *Polymer* **1987**, *28*, 1569.
(6) Cheng, L.; Shaw, H. *J. Polym. Sci.* **2000**, *38*, 747−754.
(7) Horta, A.; Fernádez-Piérola, I. *Polymer* **1981**, *22*, 783−787.
(8) Horta, A.; Fernádez-Piérola, I. *Macromolecules* **1981**, *14*, 1519−1525.
(9) Peppas, N. A.; Wu, J. C.; Meerwall, E. D. *Macromolecules* **1994**, *27*, 5626−5638.
(10) Devotta, I.; Mashelkar, R. A. *Chem. Eng. Commun.* **1996**, *156*, 31−45.
(11) Papanu, J. S.; Soane, D. S.; Bell, A. T.; Hess, D. W. *J. Appl. Polym. Sci.* **1989**, 38, 859−885.
(12) Masaro, L.; Zhu, X. X. *Prog. Polym. Sci.* **1999**, *24*, 731−775.
(13) Vieth, W. R. In *Diffusion In and Through Polymers. Principles and Applications*; Oxford University Press: New York, 1991.
(14) Hassan, M. M.; Durning, C. J.; Tong, H. M.; Lee, K. W. In *Polymer Surfaces and Interfaces: Characterization, Modification and Application*; Mittal, K. L., Lee, K. W., Eds.; VSP: Utrech cjd, The Netherlands, 1996.
(15) Hassan, M. M.; Durning, C. J. *J. Polym. Sci., Part B: Polym. Phys.* **1999**, *37*, 3159−3171.
(16) Ugur, S.; Pekcan, Ö. *Polym. Int.* **1999**, *48*, 485−490.
(17) Ugur, S.; Pekcan, Ö. *Polymer* **2000**, *41*, 1571−1575.

(18) Pekcan, Ö.; Ugur, S. *J. Appl. Polym. Sci.* **1999**, *74*, 948−957.
(19) Sammon, C.; Yarwood, J.; Everall, N. *Polymer* **2000**, *41*, 2521−2534.
(20) Hyde, T. M.; Gladden, L. F. *Polymer* **1998**, *39*, 811−819.
(21) O'Neil, G. A.; Torkelson, J. M. *Macromolecules* **1997**, *30*, 5560−5562.
(22) Koenig, J. L.; Snively, C. M. *Spectroscopy* **1998**, *13*, 22.
(23) Brandrup, J.; Immergut, E. H.; Grulke, E. A. In *Polymer Handbook*; John Wiley & Sons: New York, 1999; pp 501−502.
(24) Challa, S. R.; Wang, S.-Q.; Koenig, J. L. *Appl. Spectrosc.* **1996**, *50*, 1339.
(25) Shimizu, S.; Aiki, Y.; Kurita, K.; Furusaka, M. *Physica B* **1998**, *241−243*, 1032−1034.
(26) Ribar, T.; Bhargava, R.; Koenig, J. L. *Macromolecules* **2000**, *33*, 8842−8849.
(27) Ribar, T.; Koenig, J. L. *Macromolecules* **2001**, *34*, 8340−8346.
(28) Beerbower, A.; Dickey, J. R. *Am. Soc. Lubr. Eng. Trans.* **1969**, *12*, 1.
(29) Cooper, W. J.; Krasicky, P. D.; Rodriguez, F. *J. Appl. Polym. Sci.* **1986**, *31*, 65−73.

MA020401U